

# Research article

## Characterisation of semi-volatile hydrocarbon emissions from diesel engines

Amanda S. Mahlangu<sup>1</sup>, Paul W. Schaberg<sup>2</sup>, Mark C. Wattrus<sup>2</sup>, Patricia B.C. Forbes<sup>1\*</sup>

<sup>1</sup>Department of Chemistry, Faculty of Natural and Agricultural Sciences, University of Pretoria, Pretoria 0002, South Africa, Email: patricia.forbes@up.ac.za, Email: amanda.mahlangu85@gmail.com

<sup>2</sup>Sasol Energy, Sasol Fuels Application Centre, Bridge Place, Capricorn Park, Cape Town, 7945, South Africa

Received: 26 November 2019 - Reviewed: 16 January 2020 - Accepted: 13 February 2020

<https://doi.org/10.17159/caj/2020/30/1.7672>

### Abstract

Exhaust emissions from diesel vehicles have recently been receiving global attention, due to potential human health effects associated with exposure to emitted pollutants. In addition, a link has recently been established between unburnt hydrocarbon (HC) emissions from diesel engines and photochemical smog. Despite being present at very low concentrations in the exhaust, these HCs may act as precursors in the formation of photochemical smog pollution. While short-chain HCs are easier to characterise and have been successfully reduced in many developed cities, longer chain HCs, most likely arising from diesel exhaust emissions, have been poorly quantified to date, and a limited range of HCs from this source has been studied. In this study, transient cycle tests were conducted to collect exhaust emissions from a Euro 3 compliant, 1.6 L test engine fuelled with three diesel fuels; a highly paraffinic fuel, a South African market fuel and a European reference fuel. Portable denuder samplers were used to collect the emissions and analysis was done by thermal desorption-comprehensive 2D gas chromatography-time of flight mass spectrometry (TD-GC x GC-TofMS). The South African market diesel had the greatest n-alkane emissions, with greater emissions observed in the earlier phases (low and medium phase) of the WLTC test cycle. The total n-alkane emissions for this fuel ranged from 34.80 mg/km - 282.67 mg/km from the low to the extra-high phase. The paraffinic diesel had the second highest n-alkane emissions with the total emissions ranging from 35.43 mg/km - 164.99 mg/km. The European reference diesel had the lowest n-alkane emissions amongst the three fuels, with the total emissions ranging from 22.46 mg/km - 82.56 mg/km. Substituted alkyl-benzenes were also detected in the gas phase emissions from each fuel, however only semi-quantitative analysis of these compounds was conducted. The results showed that long-chain HCs were present at easily detectable concentrations in diesel engine exhaust emissions, which is critical in understanding their contribution to photochemical ozone and informing appropriate mitigation and management strategies.

### Keywords

Photochemical smog, hydrocarbons, ozone, diesel exhaust emissions, ozone formation potential, emission factor

## Introduction

Exhaust fumes from vehicular emissions are one of the biggest contributors to pollution of the ambient atmosphere, which could be of great concern for South Africa's agricultural sector and in urban environments. Photochemical smog is produced in the atmosphere from the reaction of nitrogen oxides (NO<sub>x</sub>) and volatile organic compounds (VOCs), in the presence of ultraviolet sunlight. This complex process occurs in the lower atmosphere (troposphere) and results in the formation of photochemical ozone (O<sub>3</sub>), the principal component associated with photochemical smog. The Southern African region is characterised by numerous sources of ozone-forming compounds and presents ideal environmental conditions for O<sub>3</sub> formation. The most significant pollutants from vehicular emissions include nitrogen oxides (NO<sub>x</sub>) and HCs which are key precursors to photochemical smog formation. Whilst both

diesel and petrol engines contribute to NO<sub>x</sub> emissions, until recently the latter was thought to be the primary source of HC emissions in the atmosphere. Characterisation studies on airborne organic compounds in the USA show that there is a significant contribution of semi-volatile organic compounds (SVOCs) emanating from diesel exhaust, to the atmosphere's non-methane organic gas (NMOG) load (Jathar et al., 2014). Gaseous diesel exhaust HCs are composed predominantly of alkanes (straight, branched and cycloalkanes), aromatics (alkyl-benzenes and 2-5 ring polycyclic aromatic hydrocarbons) and alkenes (Gentner et al., 2012, Storey et al., 1999). Although the South African vehicle fleet is dominated by petrol cars, the National Association of Automobile Manufacturers of South Africa (NAAMSA) has reported a steady increase in the popularity of diesel engine models over recent years (Energy, 2017).

SVOCs are described as compounds with an effective saturation concentration ( $C^*$ ) of  $0.1 \mu\text{g m}^{-3}$  –  $1000 \mu\text{g m}^{-3}$  which corresponds to a vapour pressure range of  $10^{-8}$ – $10^{-2}$  Torr (Robinson et al., 2007). These compounds tend to partition between the particulate and gaseous phases at high atmospheric dilution, and thus may participate in gas phase photochemical reactions.

Numerous studies have reported that long term exposure to PM emissions may cause cardiovascular and respiratory diseases, whilst the organic compounds adsorbed onto the surface of PM are toxic and carcinogenic (Reşitoğlu et al., 2015, Kagawa, 2002, Wichmann, 2007). The detrimental health and environmental impacts of photochemical  $\text{O}_3$  such as eye irritation, a decline in respiratory function, reduced visibility and damage to crops and vegetation (Laban et al., 2018) has also been reported in literature. According to the South African National Ambient Air Quality Standards for Criteria pollutants (2009 and 2012), the 8-hourly running average standard for  $\text{O}_3$  is  $120 \mu\text{g/m}^3$  (61 ppb), however numerous exceedances have been observed in various regions in South Africa. A study by Zunckel et al. monitored surface ozone outside urban areas in Southern Africa and found that the highest  $\text{O}_3$  concentrations were over Botswana and the Mpumalanga Highveld (Zunckel et al., 2004). Both regions had highs between 40 and 60 ppb, however the average concentration in October 2000 was greater than 90 ppb. Gautam et al. speciated diesel exhaust emissions under steady state conditions (Gautam et al., 1996). The ozone formation potential (OFP) of speciated alkyl-benzenes ranged from 0.406 - 0.767  $\text{mg O}_3/\text{bhp-hr}$  for ethylbenzene and 1,2,4-trimethylbenzene respectively and OFP values of 0.119  $\text{mg/bhp-hr}$  and 0.018  $\text{mg/bhp-hr}$  were reported for octane and nonane respectively, where bhp-hr is brake horsepower-hour. In another study by Olumayede, the contribution of individual VOCs to photochemical ozone formation in Southern Nigeria was studied (Olumayede, 2014). The following photochemical  $\text{O}_3$  formation potentials were reported:  $25.7 \mu\text{g/m}^3$  for m,p-xylene,  $11.02 \mu\text{g/m}^3$  for ethylbenzene,  $26.43 \mu\text{g/m}^3$  for undecane,  $18.85 \mu\text{g/m}^3$  for 1,2,4-trimethylbenzene and  $12.27 \mu\text{g/m}^3$  for toluene. It is evident that the contribution of different HC species to  $\text{O}_3$  formation varies within chemical classes and between HCs of different classes.

Detailed mechanisms underlying the photochemical conversion of precursor compounds to photochemical ozone have not been elucidated, however, the key elements can be explained using generalized reaction mechanisms. Smog chamber irradiation studies have also been conducted to investigate ozone formation as a function of the initial concentration of its precursors. These studies show that reducing HC and  $\text{NO}_x$  concentrations simultaneously leads to a decrease in  $\text{O}_3$ , however, this is less than the decrease observed from HC reduction alone (Glasson, 1981). Thus historically it has been known that by controlling HC levels in the atmosphere,  $\text{O}_3$  reduction could be achieved in urban areas (Glasson, 1981). In recent years, VOC emissions have been successfully quantified and reduced in many developed cities, however, research shows that longer chain HCs are typically not considered as part of air

quality control strategies. A study was conducted using high resolution measurements to investigate the abundance of diesel related HCs in the atmosphere at an urban background site in London and a comparison of these results to the emission inventory data showed that there is a drastic underestimation of the impact of diesel related emissions on urban air quality (Dunmore et al., 2015).

The challenge faced when characterising SVOCs stems from difficulties in quantitative collection and chemical analysis of these species. Traditional sampling methods for gaseous-particulate phase analytes employ high volume samplers that make use of a glass fibre filter that removes particles from the sample flow, and an adsorbent such as Tenax or polyurethane foam (PUF), to adsorb the gas phase analytes downstream of the filter (Geldenhuis et al., 2015). Although such high volume samplers are robust and easy to use in the field, they exhibit inherent limitations due to the sampling configuration and high volumetric flow rate (Forbes and Rohwer, 2015). Another commonly used sampling method, particularly when conducting engine tests, is collection of dilute exhaust emissions into Tedlar® bags from a constant volume sampler (CVS) and subsequent analysis of emissions by gas chromatography-mass spectrometry (GC-MS). This sampling method is adequate for sampling of VOCs, however, heavier compounds tend to condense on the walls of the sampling bags, which results in errors during quantitative analyses (Newkirk et al., 1993).

Denudation, a sampling technique that has been used extensively for air monitoring applications, eliminates two major limitations suffered by high volume samplers. By removing SVOC gas phase analytes prior to downstream collection of the particulate matter, it prevents adsorption of the gas phase analytes onto particulate matter collected on the filter or onto the filter medium itself. The second artefact relates to volatilisation of the particle phase analyte from the filter. During denudation, a second gas phase sampling device is placed downstream of the filter, which collects any “blow-off” from the filter (Forbes and Rohwer, 2015). Furthermore, denuders allow for collection of diluted exhaust samples, without the need to collect large volumes of samples, as analytes are stripped from the air sample and pre-concentrated onto the sorbent, which later may be extracted or introduced directly into the analytical instrument during analysis.

In this study, an emissions monitoring campaign was conducted to collect and characterise diesel exhaust emissions from a diesel test engine which is a popular model for the passenger car fleet on South African roads. Simulated vehicle exhaust emission testing was conducted at a controlled engine test cell facility using a standard emission test cycle. Cold-start emission tests were performed for three different fuels. Simultaneous sampling of gaseous and particulate exhaust emissions was achieved by using denuder sampling devices with thermal desorption-comprehensive two dimensional gas chromatography-time of flight mass spectrometry (TD-GC x GC-TofMS) analysis. Here we report on these gas phase n-alkane and aromatic hydrocarbon

diesel emissions and their related ozone formation potentials which can be estimated by assigning maximum incremental reactivity (MIR) indices to each compound.

## Experimental

### Test engine and Test fuels

Simulated vehicle emissions testing was conducted in a test cell (Fig 1) with a Euro 3 compliant, 1.6 L test engine, which was fitted with a close-coupled diesel oxidation catalyst (DOC).



**Figure 1:** Test cell setup

The engine had completed ~137 hours of running on the test bed, under varied operating conditions. A complete set of diagnostic

checks were carried out on the engine before testing commenced to ensure that it was performing according to specification. The test engine was coupled to an electrical engine dynamometer which uses a mathematical model to simulate engine operation during emissions testing. Figure 1 shows the test cell setup. Three diesel fuels were selected for testing: a highly paraffinic diesel fuel complying with the European EN15940 specification (PAR10), a South African market fuel complying with the South African SANS 342 specification (SAM10), and a reference fuel complying with the European EN590 specification (EUR10). All of the fuels contained less than 10 ppm sulphur, and were chosen because of their distinct compositional characteristics. The dynamometer details and fuel specifications are listed in Table 1 and Table 2 respectively.

**Table 1:** Dynamometer details

Make and model	Horiba Dynas3 LI350
Rated power and torque	350 kW, 750 Nm
Control system	Horiba SPARC controller and Horiba STARS test automation system

### Test cycle

The World Harmonized Light vehicle Test Cycle (WLTC) was used for emissions testing. Figure 2 illustrates a typical speed profile of this test cycle. It consists of four characteristic speed phases (low, medium, high and extra high), and emissions from each phase were collected onto separate samplers.

**Table 2:** Fuel properties and composition

Analysis	Method	Sasol 10ppm	EN590	GTL
Sulfur, mg/kg	ASTM D5453	5	<1	<1
Density, kg/l @ 20 °C	ASTM D4052	0.8163	0.8328	0.7650
Flash Point, °C	ASTM D93	63.9	83.0	57.0
Distillation, °C				
Initial Boiling Point		176.8	193.1	150.6
5%		187.0	207.1	173.9
10%	ASTM D86	192.4	218.1	184.3
50%		232.8	277.0	262.8
90%		333.5	333.0	338.6
95%		368.2	347.9	352.4
Final Boiling Point		389.1	355.6	356.7
Cetane number	ASTM D6890	49.7	53.8	80.0
Viscosity, cSt @ 40°C	ASTM D445/D7042	2.06	2.79	2.20
N-paraffins		24.5	9.4	51.9
Branched paraffins		24.1	39.9	47.7
Monocyclic Paraffins		14.0	16.8	0.2
Bi- and polycyclic paraffins		9.2	4.7	0.2
Alkyl benzenes	GC X GC (mass %)	10.9	13.2	0.0
Cyclic alkylbenzenes		14.9	9.1	0.0
Bi- and polycyclic aromatics		2.3	6.9	0.0
Sum		99.9	100.0	100.0

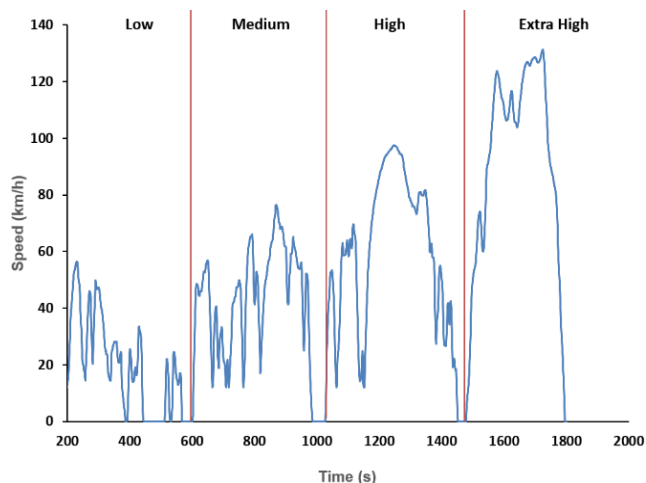


**Figure 2:** Speed profile of the WLTC test cycle used during emissions testing.

## Emissions sampling and instrumental analysis

Exhaust gas was drawn directly from the engine's exhaust pipe and fed into a mini dilution tunnel (Horiba MDLT-1303T). The diluted exhaust was sampled onto denuder samplers consisting of a quartz fibre filter sandwiched between two multi-channel polydimethylsiloxane (PDMS) traps (Forbes et al., 2012) via a four-way flow splitter at the exit of the dilution system. Portable sampling pumps (GilAir plus, Sensidyne) were used to draw the diluted exhaust through the denuders at a sampling rate of 500 mL/min. Samples were collected in duplicate for each fuel after which the test fuel was changed.

During fuel change-over the fuel supply system was flushed with approximately 10 litres of the new fuel to remove the remaining old fuel. This was then followed by a 60 min run where the engine was operated at mid-load conditions (50% of full load), at 2500 rpm for an hour. The engine was then pre-conditioned with the new fuel by running the test cycle once, followed by a 20 min run at mid-load conditions, at 2500 rpm once again. The engine was then shut down, and left un-operated overnight, allowing it to stabilize to ambient temperature.

After sampling, each PDMS trap was end capped, wrapped in Al foil and each quartz fibre filter was placed in a clean amber vial. Samples were placed in zip lock bags and refrigerated at -18 °C until analysis using a LECO Pegasus 4D TD-GC x GC-TofMS system with an internal standard mix containing hexadecane-d34, naphthalene-d8 and phenanthrene-d10 in hexane.

## Hydrocarbon speciation

Identification of target aromatic and alkane HCs was achieved by matching retention times to those of authentic reference standards (C8-C20 n-alkane standard from Sigma-Aldrich and DHA-aromatic standard from Restek) and calculated retention indices, as well as mass spectral matching using the NIST MS search mass spectral library. Quantitation of n-alkane HCs was achieved by linear regression analysis. Six concentrations (1, 5, 10, 20, 30 and 60 ng/ $\mu$ L) of the C8-C20 alkane standard mix were

prepared in hexane (99%, Sigma-Aldrich) and each standard was spiked onto a pre-conditioned trap and analysed in duplicate on the TD-GC x GC-TofMS.

To calculate the emission factor (ng/km) of each n-alkane the mass obtained from calibration (ng) was corrected using dilution factors which were measured continuously during emissions testing.

## Results and Discussion

### N-alkane gas phase emissions

Transient cycle tests were performed for all three fuels from a cold engine start, over each phase of the WLTC test. Figure 3 shows the relative n-alkane emission factors of each fuel for each phase of the WLTC cycle. The SAM10 diesel had the greatest n-alkane emissions with greater emissions observed in the low phase of the WLTC cycle, and PAR10 diesel had the second highest n-alkane emissions. The EUR10 diesel had the lowest n-alkane emissions amongst the three fuels which may be attributed to its low n-paraffin fuel content, and, potentially its lower volatility. Although PAR10 diesel has the highest n-paraffin fuel content, it had lower n-alkane emissions than the SAM10 diesel. This could be as a result of the high cetane number of this fuel compared to that of the SAM10 fuel. A higher cetane number means the fuel ignites easily which results in better fuel combustion and thus reduction of harmful emissions from unburnt HCs (Ladommatos et al., 1996). A correlation between HC emissions and cetane number has been demonstrated for diesel engine emissions where a reduction in HC emissions was observed with increasing cetane number (Bartlett et al., 1992).

From Figure 3, although unexpectedly higher emissions were observed during the high phase of the WLTC cycle, a general decrease in emissions was observed from the "Low" phase to the "Extra high" phase. This is a result of an increase in the engine and exhaust catalyst temperature which results in improved combustion conditions and catalytic oxidation during engine operation.

### Aromatic hydrocarbon gas phase emissions

Semiquantitative analysis of the test fuel emissions was also conducted to identify target aromatic HCs. The target list contained 30 alkyl-benzenes. Figure 4 shows the relative gas phase alkyl-benzene emission factors of each fuel for each phase of the WLTC cycle. It is evident that the EUR10 fuel had the highest alkyl-benzene hydrocarbon emissions, followed by the SAM10 fuel and PAR10 fuel respectively. This trend was highly consistent with the fuel composition, as the EUR10 fuel has the highest alkyl-benzene fuel content and the SAM10 fuel the second highest.

Alkyl-benzene emissions were seen for the PAR10 fuel, although this fuel contains no alkyl-benzenes, thus emissions were suspected to be from residual alkyl-benzene emissions from the previous combustion of other fuels. To further investigate this, a

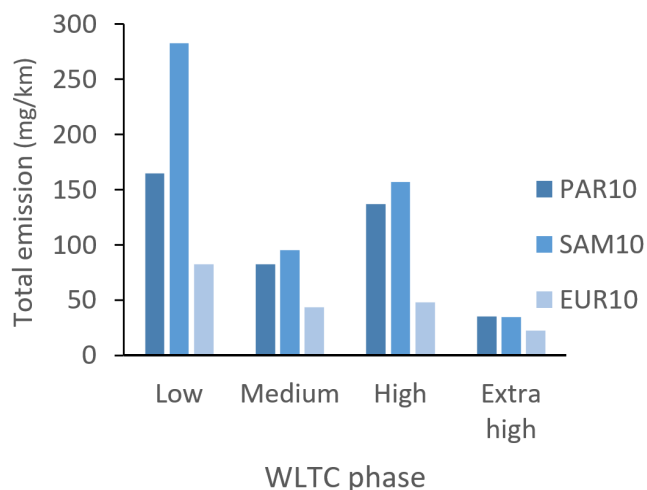


Figure 3: Relative gas phase n-alkane cold start emissions summed up for each of the WLTC test cycle phases, for each test fuel.

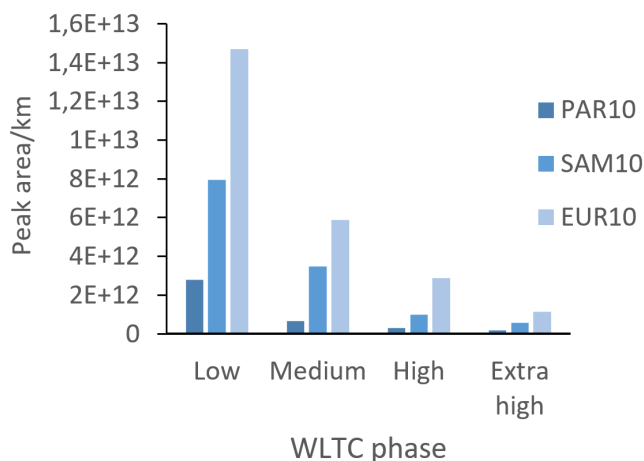


Figure 4: Relative gas phase alkyl-benzene cold start emissions summed up for each of the WLTC test cycle phases, for each test fuel.

qualitative analysis of the background samples was conducted. Background samples were taken with the engine switched off, however, the dilution ratio was kept constant to maintain the volume of incoming dilution air. Analysis of these samples confirmed that most of the target alkyl-benzenes were present at low levels in the background air.

Figure 5 shows a comparison of the peak areas of alkyl-benzenes identified in the emissions of the SAM10 fuel as compared to the background air.

Similar compounds to the ones reported in this study were found by other diesel exhaust characterisation studies (Alves et al., 2015, Gentner et al., 2013, Schauer et al., 1999). Comparing the emission factors however can be challenging as the emission factors of hydrocarbons from mobile sources have been shown to depend on engine design, engine operation and fuel composition (Cross et al., 2015), amongst other factors.

### Effect of the exhaust after-treatment systems

To meet the increasingly stringent air quality limits regarding

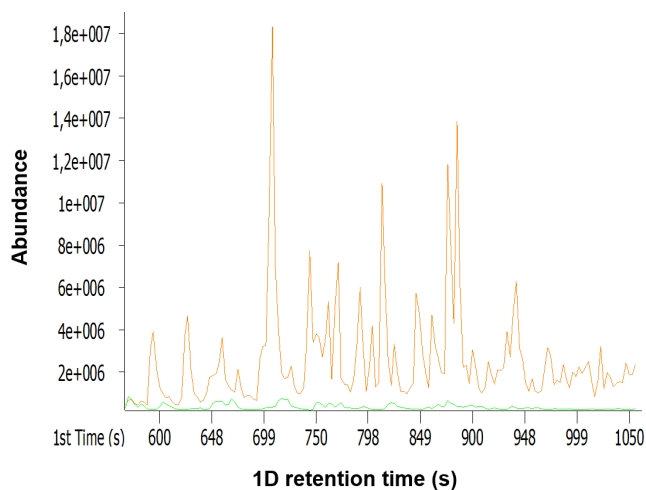


Figure 5: Example extracted ion chromatograms ( $m/z = 91$ ) showing the gas phase aromatic hydrocarbon emissions from SAM10 diesel cold start Phase 1 (top) as compared to the background air (bottom).

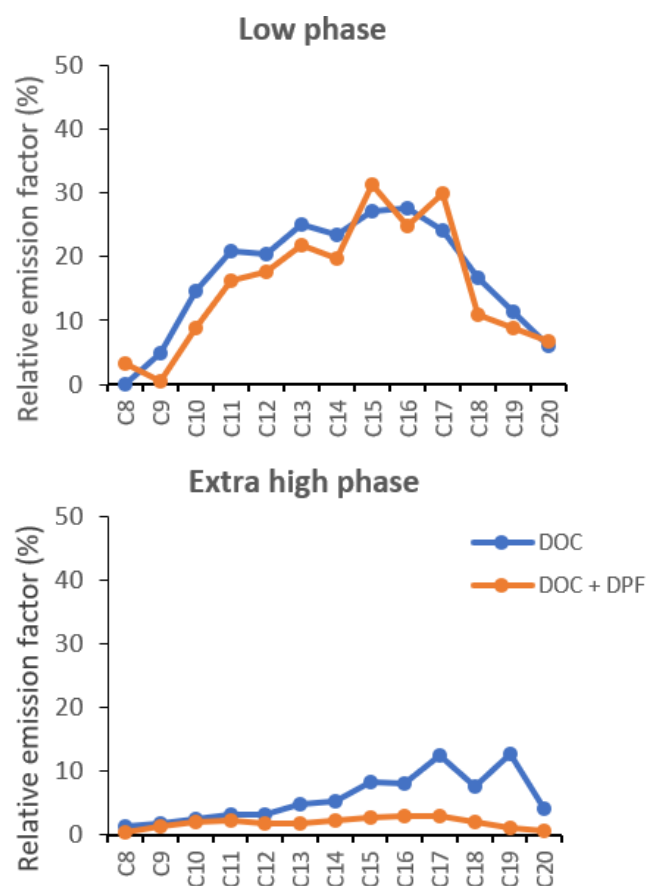


Figure 6: Preliminary relative gaseous n-alkane emission factors for the DOC and DOC+DPF exhaust after-treatment configurations.

vehicular exhaust emissions, modern day diesel vehicles have exhaust after-treatment systems, which may include a diesel oxidation catalyst (DOC), diesel particulate filter (DPF) and/or a selective catalytic reduction (SCR) system. To investigate the effect of the exhaust after-treatment system, emissions tests were performed using two configurations: DOC and DOC-DPF. Figure 6 shows the n-alkane relative emission factors for both configurations, during the low phase of the WLTC cycle.



**Figure 7:** Quartz fibre filters used to collect particulate emissions for the EUR10 fuel during the low phase of the WLTC test cycle with the DOC only (left) and the DOC-DPF (right) in-line.

The relative emission factors (%) were determined by expressing the emission factor of each n-alkane relative to that of the n-alkane with the highest emission factor ( $\equiv 100$ ). The results show a decrease in emissions from the low phase to the extra-high phase, which can be attributed to oxidation of gaseous hydrocarbon emissions by the DOC during high engine temperatures. The results also show lower emissions for the DOC-DPF configuration as compared to the DOC configuration. This was attributed to additional oxidation of HCs by precious metals found within the DPF as well as removal of hydrocarbons adsorbed onto the surface of particulate matter by the DPF.

Figure 7 shows the effective removal of soot and PM by the DPF. These results show the importance of the exhaust after-treatment system, however, the issue remains that optimum functioning of the DOC and regeneration of the DPF requires high engine temperatures which are seldom reached during low-speed city driving conditions.

## Ozone formation potentials

The OFPs of the hydrocarbon emissions can be estimated using Carter's MIR indices which give the impact of each compound to the peak ozone concentration in a system where ozone is being formed under high  $\text{NO}_x$  concentrations, and is most sensitive to HC emissions (Carter 2010). The MIR index of each compound is given as the mass of additional ozone formed per mass of compound added to the emissions ( $\text{gO}_3/\text{gVOC}$ ). Thus using the emission factors, the OFP of each compound can then be determined from the product of the emission factor (EF<sub>n</sub>) and MIR index (MIR<sub>n</sub>) of each alkane, where n refers to the alkane with n number of carbons (equation 1).

$$\text{OFP}[\text{gO}_3/\text{km}] = \text{EF}_n [\text{gVOC}/\text{km}] \times \text{MIR}_n [\text{gO}_3/\text{gVOC}] \quad (1)$$

Photochemical smog occurs predominantly in urban areas, thus phases 1 and 2 (low and medium) cold start emissions were chosen to study the OFP of the different fuels, as they consist of low speeds which are characteristic of urban driving conditions.

The photochemical smog formation potential of n-alkane emissions from each fuel differed. A comparison of the fuel emissions revealed that the SAM10 fuel emitted more ozone forming n-alkane and aromatic HC emissions than the other two fuels. EUR10 diesel had the least n-alkane emissions, however, it had relatively high aromatic HC emissions, which contributed to the OFP of this fuel, as these compounds have large MIR indices. The PAR10 fuel had relatively high n-alkane emissions, which have low MIR factors, although high emission factors would contribute to the OFP of this fuel.

From these results, it is evident that SVOCs arising from diesel emissions have the potential to contribute to photochemical ozone formation in the atmosphere, especially in urban traffic dense areas. The comparison between the test fuels cannot be regarded as conclusive, however, as diesel fuels also contain significant concentrations of branched and cyclic paraffins, which were not quantified in this study.

## Conclusion

SVOC exhaust emissions from a diesel engine used in light-duty passenger vehicles were characterised for three fuels. The engine was operated over the WLTC driving cycle consisting of low, medium, high, and extra high speed phases. HC (n-alkane and aromatic) gas phase emissions arising from each fuel were then determined for each phase of the test cycle. The three test fuels showed differing levels of n-alkane and aromatic SVOC emissions, and hence their OFP differed, which could tentatively be explained by the physical and chemical characteristics of the fuels. A general decrease in n-alkane emissions was observed for each fuel when moving from the "Low" to the "Extra high" speed phase of the test cycle, and lower gas phase hydrocarbon emissions were observed in the presence of a DOC and DPF combination. This was attributed to increased engine temperatures which result in improved combustion conditions and optimal functioning of the DOC and DPF. Monitoring of semi-volatile HC emissions may be critical in understanding elevated ozone levels in urban areas, which are often higher than model predictions. This study has illustrated the successful use of denuders and comprehensive 2D gas chromatography with mass spectrometric detection to collect and characterise semi-volatile n-alkane and aromatic emissions from diesel exhaust. Such studies are important in better understanding the tropospheric ozone levels in South Africa and in informing air quality management practices.

## Acknowledgements

The Sasol Fuels Application Centre is acknowledged for granting the use of the engine test cell facility and resources provided. Thanks to Mr. David Masemula for construction of PDMS traps and Dr. Yvette Naudé for assistance during instrumental analysis. Financial support from Sasol and the National Research Foundation (NRF) is highly appreciated.

NOTE: An earlier version of this paper was presented at the National Association of Clean Air (NACA) Conference and was published in its Proceedings.

## References

- Alves, C. A., Lopes, D. J., Calvo, A. I., Evtyugina, M., Rocha, S. & Nunes, T. 2015. Emissions from light-duty diesel and gasoline in-use vehicles measured on chassis dynamometer test cycles. *Aerosol Air Qual. Res.*, 15, 99-116.
- Bartlett, C., Betts, W., Booth, M., Giavazzi, F., Guttman, H., Heinze, P. & Mayers, R. 1992. Diesel Fuel Aromatic Content and Its Relationship with Emissions from Diesel Engines. Congawe report no. 92/54.
- Carter, W. Updated Maximum Incremental Reactivity Scale and Hydrocarbon Bin Reactivities for Regulatory Applications. 2010. *California Air Resources Board Contract*. 07e339.
- Cross, E. S., Sappok, A. G., Wong, V. W. & Kroll, J. H. 2015. Load-dependent emission factors and chemical characteristics of IVOCs from a medium-duty diesel engine. *Environmental Science & Technology*, 49, 13483-13491.
- Dunmore, R., Hopkins, J., Lidster, R., Lee, J., Evans, M., Rickard, A., Lewis, A. & Hamilton, J. 2015. Diesel-related hydrocarbons can dominate gas phase reactive carbon in megacities. *Atmospheric Chemistry and Physics*, 15, 9983-9996.
- Ratshomo, K. & Nemahe, R. 2017. Overview of the Petrol and Diesel Market in South Africa between 2007 and 2016. Available [Online]: <http://www.energy.gov.za/files/media/explained/Overview-of-Petrol-and-Diesel-Market-in-SA-between-2007-and-2016.pdf> [Accessed 2019].
- Forbes, P. B., Karg, E. W., Zimmermann, R. & Rohwer, E. R. 2012. The use of multi-channel silicone rubber traps as denuders for polycyclic aromatic hydrocarbons. *Analytica Chimica Acta*, 730, 71-79.
- Forbes, P. B. & Rohwer, E. R. 2015, Chapter 5: Denuders, in *Comprehensive Analytical Chemistry vol. 70: Monitoring of Air Pollutants: Sampling, Sample Preparation and Analytical Techniques*, Patricia Forbes (ed.), pp. 153-181, Elsevier, Netherlands.
- Gautam, M., Gupta, D., El-Gazzar, L., Lyons, D. W. & Popuri, S. 1996. Speciation of heavy duty diesel exhaust emissions under steady state operating conditions. *SAE Transactions*, 2337-2364.
- Geldenhuis, G., Rohwer, E. R., Naudé, Y. & Forbes, P. B. 2015. Monitoring of atmospheric gaseous and particulate polycyclic aromatic hydrocarbons in South African platinum mines utilising portable denuder sampling with analysis by thermal desorption-comprehensive gas chromatography-mass spectrometry. *Journal of Chromatography A*, 1380, 17-28.
- Gentner, D. R., Isaacman, G., Worton, D. R., Chan, A. W., Dallmann, T. R., Davis, L., Liu, S., Day, D. A., Russell, L. M. & Wilson, K. R. 2012. Elucidating secondary organic aerosol from diesel and gasoline vehicles through detailed characterization of organic carbon emissions. *Proceedings of the National Academy of Sciences*, 109, 18318-18323.
- Gentner, D. R., Worton, D. R., Isaacman, G., Davis, L. C., Dallmann, T. R., Wood, E. C., Herndon, S. C., Goldstein, A. H. & Harley, R. A. 2013. Chemical composition of gas-phase organic carbon emissions from motor vehicles and implications for ozone production. *Environmental Science & Technology*, 47, 11837-11848.
- Glasson, W. A. 1981. Effect of Hydrocarbon and NO<sub>x</sub> on Photochemical Smog Formation under Simulated Transport Conditions. *Journal of the Air Pollution Control Association*, 31, 1169-1172.
- Jathar, S. H., Gordon, T. D., Hennigan, C. J., Pye, H. O., Pouliot, G., Adams, P. J., Donahue, N. M. & Robinson, A. L. 2014. Unspeciated organic emissions from combustion sources and their influence on the secondary organic aerosol budget in the United States. *Proceedings of the National Academy of Sciences*, 111, 10473-10478.
- Kagawa, J. 2002. Health effects of diesel exhaust emissions—a mixture of air pollutants of worldwide concern. *Toxicology*, 181, 349-353.
- Laban, T. L., Van Zyl, P. G., Beukes, J. P., Vakkari, V., Jaars, K., Borduas-Dedekind, N., Josipovic, M., Thompson, A. M., Kulmala, M. & Laakso, L. 2018. Seasonal influences on surface ozone variability in continental South Africa and implications for air quality. *Atmospheric Chemistry and Physics*, 18, 15491-15514.
- Ladommatos, N., Parsi, M. & Knowles, A. 1996. The effect of fuel cetane improver on diesel pollutant emissions. *Fuel*, 75, 8-14.
- Newkirk, M. S., Smith, L. R. & Merritt, P. M. 1993. Heavy-duty diesel hydrocarbon speciation: key issues and technological challenges. *SAE Technical Paper* 932853.
- Olumayede, E. G. 2014. Atmospheric volatile organic compounds and ozone creation potential in an urban center of southern Nigeria. *International Journal of Atmospheric Sciences*. Article ID 764948 <https://doi.org/10.1155/2014/764948>
- Reşitoğlu, İ. A., Altinişik, K. & Keskin, A. 2015. The pollutant emissions from diesel-engine vehicles and exhaust aftertreatment systems. *Clean Technologies and Environmental Policy*, 17, 15-27.
- Robinson, A. L., Donahue, N. M., Shrivastava, M. K., Weitkamp, E. A., Sage, A. M., Grieshop, A. P., Lane, T. E., Pierce, J. R. & Pandis, S. N. 2007. Rethinking organic aerosols: Semivolatile emissions and photochemical aging. *Science*, 315, 1259-1262.

---

Schauer, J. J., Kleeman, M. J., Cass, G. R. & Simoneit, B. R. 1999. Measurement of emissions from air pollution sources. 2. C1 through C30 organic compounds from medium duty diesel trucks. *Environmental Science & Technology*, 33, 1578-1587.

Storey, J. M., Domingo, N., Lewis, S. A. & Irick, D. K. 1999. Analysis of semivolatile organic compounds in diesel exhaust using a novel sorption and extraction method. *SAE Technical Paper* 1999-01-3534.

Wichmann, H.-E. 2007. Diesel exhaust particles. *Inhalation Toxicology*, 19, 241-244.

Zunckel, M., Venjonoka, K., Pienaar, J., Brunke, E., Pretorius, O., Koosiale, A., Raghunandan, A. & Van Tienhoven, A. 2004. Surface ozone over southern Africa: synthesis of monitoring results during the Cross border Air Pollution Impact Assessment project. *Atmospheric Environment*, 38, 6139-6147.